UNIVERSIDADE DE LISBOA
FACULDADE DE CIÊNCIAS
DEPARTAMENTO DE BIOLOGIA VEGETAL

Uncovering the role of host Cullin 3 during *Plasmodium berghei* liver stage infection

Gabriela Stephanie Peres Cristo

DISSERTAÇÃO DE MESTRADO EM BIOLOGIA MOLECULAR E GENÉTICA

2014

UNIVERSIDADE DE LISBOA
FACULDADE DE CIÊNCIAS
DEPARTAMENTO DE BIOLOGIA VEGETAL

Uncovering the role of host Cullin 3 during *Plasmodium berghei* liver stage infection

Gabriela Stephanie Peres Cristo

Dissertação orientada pela Doutora Vanessa Alexandra Zuzarte Luís (IMM)
e pela Professora Doutora Rita Maria Pulido Garcia Zilhão (FCUL)

DISSERTAÇÃO DE MESTRADO EM BIOLOGIA MOLECULAR E GENÉTICA

2014

ACKNOWLEDGEMENTS

À Deus, obrigada por me abençoar e me capacitar até aqui.

À Dr[a]. Maria Mota, pela oportunidade e por acolher-me tão bem em seu laboratório.

À Dr[a]. Vanessa Luíz, obrigada pelos ensinamentos, durante as reuniões; pela disponibilidade; paciência; pela sua dedicação e confiança!

À prof[a]. Dr[a]. Rita Zilhão, obrigada pela disponibilidade ao longo deste ano e por se preocupar com o meu percurso.

À Lénia ("minha madrinha do Lab"), obrigada pela ajuda, pela amizade, pelos preciosos conselhos e ensinamentos.

Aos meus colegas do mestrado de BMG-2012.

Aos professores pelos ensinamentos compartilhados.

Aos meus colegas da Unidade da Malária. Obrigado pelo respeito, apoio, bom humor e brincadeiras sadias, intercaladas por trabalho realizado com seriedade. Em especial, agradeço ao João Oliveira, Márcia Medeiros, Margarida Ruivo, Ana Góis, Inês Alburquerque, Patrícia Meireles, Ana Parreira, Filipa Teixeira, Marta Machado, Iset e Maurice, obrigada pela ajuda, pelas conversas, amizade e apoio.

As minhas companheiras de casa, Ana Pena e Eliana, obrigada pela ajuda, companherismo, brincadeiras, força e apoio. Vocês foram fundamentais nesta etapa da minha vida!

À minha Mãe, meu porto seguro; minha melhor amiga e companheira. Obrigada pelo apoio e ensinamentos. Não há nem nunca haverá ninguém tão forte.

Ao Pedro (meu "babatwo"), obrigada pela paciência, carinho e apoio. Ès o maior!!!

Ao meu Pai e minha irmã, que mesmo distantes me apoiaram e me deram forças. Obrigada, amo vocês!!!

À minha tia Naná, obrigada por sempre acreditar que eu podia ir até ao infinito e mais além.

Aos meus amigos, próximos ou distantes. Vocês sabem que estão no meu coração.

Enfim, à todos que de alguma forma contribuiu para que fosse possível a realização deste projeto.

"For wisdom is better than corals, and all other delights themselves cannot be made equal to it."
Proverbs 8:11

RESUMO

A malária é uma das principais doenças parasitárias do mundo, sendo a causa de mais de 1 milhão de mortes todos os anos. Causada por um parasita eucariota intracelular, do género *Plasmodium*, a malária é transmitida através da picada de um mosquito fêmea do género *Anopheles*. Entre as cinco espécies que podem transmitir malária aos humanos, *Plasmodium falciparum* é o principal contribuidor para a morbilidade e mortalidade associadas à malária. O ciclo de vida do parasita é complexo e envolve um vetor, o mosquito, e um hospedeiro vertebrado. Durante o ciclo de vida no hospedeiro, existem duas fases principais: a fase hepática e a fase sanguínea. A infeção começa quando o mosquito injeta esporozoítos de *Plasmodium* na pele do hospedeiro vertebrado. Depois de atravessar a derme os parasitas entram no sistema circulatório e vão para o fígado, onde completam a fase silenciosa do seu desenvolvimento. Esta etapa de desenvolvimento assintomática acabará por levar à libertação na corrente sanguínea de milhares de novos parasitas chamados merozoítos, iniciando a fase sintomática da doença. Nos seres humanos, a fase hepática da infeção dura cerca de 6-10 dias onde o número de parasitas expande enormemente, até 40.000 vezes. Esta elevada taxa de multiplicação impõe uma necessidade significativa de nutrientes. Tal como outros agentes patogénicos intracelulares, é plausível que o parasita tenha desenvolvido mecanismos para explorar os recursos da célula hospedeira, nomeadamente o seu sistema endomembranar.

O sistema endomembranar de uma célula eucariota é composto por diferentes organelos secretores e vesículas da via endocítica. A via de endocitose desempenha um papel importante em várias funções biológicas, tais como, a absorção de nutrientes, sinalização celular, e eliminação de agentes patogénicos. No fígado, o parasita desenvolve-se rodeado por endossomas e lisossomas do hospedeiro, embora não se observe fusão e acidificação do vacúolo. Estas observações sugerem que, em vez de eliminar o parasita, as vesículas podem ter um papel importante no seu desenvolvimento durante a fase hepática. Na via endocítica, o sistema de ubiquitinação controla inúmeros processos celulares, nomeadamente na regulação da sinalização e reciclagem dos receptores de membrana. O sistema ubiquitina é uma modificação pós-tradução que consiste na ligação de uma proteína ubiquitina a um substrato. O último passo de conjugação da ubiquitina à proteína alvo é catalisado por uma enzima E3 ligase, responsável pelo reconhecimento específico dos substratos. Os *Cullin-RING ligases* (CRLs) constituem a maior classe conhecida de E3s. Os CRLs são complexos proteicos constituídos por uma proteína estrutural (Cullin), que em mamíferos é composta por uma família com seis homólogos (Cullin 1, Cullin 2, Cullin 3, Cullin 4a, Cullin 4b, e Cullin 5); uma proteína com um domínio de ligação à ubiquitina; e uma

proteína de ligação ao substrato. Estas últimas são variáveis e conferem especificidade de ligação ao substrato. Recentemente, a Cullin 3 surge como um importante regulador do tráfico vesicular, em particular na secreção e maturação dos endossomas. A depleção de Cullin 3 resulta em defeitos no transporte da carga dos endossomas para os lisossomas.

Dada a importância da associação do sistema endolisossomal durante o desenvolvimento do parasita dentro do hepatócito e o papel da Cullin 3 na via endocítica, o principal objetivo deste projeto foi avaliar o papel da Cullin 3 durante o desenvolvimento intra-hepático de *Plasmodium*. Para isso, utilizámos o modelo de roedores *Plasmodium berghei,* e realizámos ensaios funcionais de ganho ou perda de função, sobre-expressão de Cullin 3; bloqueio da ativação da Cullin 3 usando um inibidor de nedilação (MLN4924), e depleção da Cullin 3, usando siRNA.

Começámos por verificar se a sobre-expressão transiente de Cullin 3 iria causar algum efeito sobre a infeção por *Plasmodium*, bem como na acumulação de vesículas em torno do parasita. Células HeLa foram transfetadas com um plasmídeo expressando Cul3-Myc; 36 horas após a transfeção as células foram infetadas com esporozoítos de *Plasmodium berghei* que expressam *Green Fluorescent Protein* (GFP). A análise de três experiências independentes, feita por microscopia às 48 horas após a infeção, não permitiu identificar um número suficiente de células transfetadas e infetadas para poder tirar conclusões sobre o efeito da sobre-expressão da Cullin 3 na infeção por *Plasmodium*. A razão para isto foi a combinação da baixa taxa de transfeção (30%) com a extrema baixa taxa de infeção de células HeLa por *Plasmodium* (<1%).

“Nedilação” é um tipo de modificação pós-tradução de proteínas, que envolve a adição da molécula ubiquitina-NEDD8 à proteína alvo. Muitos estudos mostraram que a “nedilação" desempenha um papel importante na ativação dos *Cullin-RING ligases*. MLN4924 é uma pequena molécula inibidora da atividade da *NEDD8 activating enzyme* (NAE) que se liga a um sítio ativo designado de NEDD8-MLN4924. Como resultado, a “nedilação” das Cullins é bloqueada levando à inactivação dos complexos CRL/SCF (*Cullin-RING-ligases / Skp1-Cullin-F box proteins)* e, consequentemente, à acumulação de vários substratos dos *Cullin-RING ligases*. Logo, o próximo passo foi avaliar o bloqueio da ativação da Cullin 3 usando o inibidor da “nedilação” MLN4924, durante a infeção por *Plasmodium.* A grande vantagem do inibidor MLN4924 é a sua elevada especificidade para a inibição dos *Cullin-RING ligases*. Além disso, MLN4924 é um composto já aprovado pela FDA (*Food and Drug Administration*). Neste estudo, utilizámos células de hepatoma humanas (Huh7) que foram submetidas a 24 horas de tratamento com MLN4924 antes da infeção com parasitas

Plasmodium berghei expressando GFP. Os níveis de infeção durante a invasão e o desenvolvimento do parasita foram analisados por citometria de fluxo e microscopia. Os nossos resultados demonstraram que, aparentemente, não há efeito significativo nos níveis de infeção por *Plasmodium* durante a invasão e o desenvolvimento. No entanto, devido ao facto do tratamento das células com MLN4924 provocar expressivas alterações celulares, não pudemos determinar concretamente o efeito do bloqueio da ativação da Cullin 3 durante a infeção por *Plasmodium*.

Para avaliar o papel da Cullin 3 durante a infeção por *Plasmodium* de uma forma mais específica, utilizámos *short interfering RNA* (siRNA) para causar a depleção da Cullin 3 em células Huh7. As células foram transfetadas com siRNA para a Cullin 3, e após 36 horas de depleção foram infetadas com parasitas expressando GFP. Os níveis de infeção foram analisados por *Quantitative real-time reverse transcription polymerase chain reaction* (qRT-PCR) e microscopia. Os resultados obtidos após 48 horas de infeção sugerem que a depleção da Cullin 3 por siRNA provoca uma redução do número de células infetadas com *Plasmodium.*

Em conclusão, os nossos resultados demonstram que o composto MLN4924 não tem efeitos significativos durante a infeção por malária na fase hepática. Além disso, este inibidor apresenta demasiados efeitos adversos sobre as células hospedeiras, de modo que, a interpretação dos resultados não é conclusiva. No entanto, os resultados da depleção da Cullin 3 sugerem que esta pode ser relevante para a infeção por *Plasmodium*, uma vez que a depleção da sua expressão por siRNA reduz a carga parasitária. Contudo, mais experiências serão necessárias para elucidar os mecanismos moleculares por detrás deste efeito. As experiências realizadas não demonstraram qualquer efeito significativo na acumulação de vesículas em torno do parasita. Estas observações podem ser explicadas pelo facto do papel exato da ubiquitinação mediada por Cullin 3 na via endocítica permanecer ainda desconhecido. Esta proteína pode estar envolvida em cada uma das etapas da maturação dos endossomas, que incluem, alterações morfológicas, troca de componentes de membrana, movimento do endossoma para a região perinuclear, e formação de *intraluminal vesicles* (ILVs). Assim, um melhor conhecimento dos intervenientes moleculares que afetam direta ou indiretamente os processos de maturação do endossoma será importante para esclarecer a interação entre o parasita e a célula hospedeira, e contribuir para o desenvolvimento de novas estratégias para controlar a infeção por malária na fase hepática.

Palavras-chave: Malária, Cullin 3; via endocítica; fase hepática; infeção por *Plasmodium.*

ABSTRACT

Malaria is caused by *Plasmodium* parasites and transmitted by infected female *Anopheles* mosquitoes. There are two stages of malaria infection in mammals. The first stage occurs in the liver, where *Plasmodium* sporozoites invade and replicate extensively inside hepatocytes. This high multiplication rate imposes a significant demand of nutrients and therefore it is likely that *Plasmodium* has developed mechanisms to exploit the host cell resources. Recent studies established that interactions between *Plasmodium berghei* parasites and the host endocytic pathway are crucial for parasite growth during liver stage infection. Cullin 3 recently emerged as an important regulator of intracellular trafficking, in particular secretion and endosome maturation. Cullin 3 is specifically activated (neddylated) at the plasma membrane and is found associated with vesicular markers for intracellular trafficking. Additionally, depletion of Cullin 3 results in deformation of late endosomes and causes defects in the transport of endocytic cargo to lysosomes. Given the important association of host vesicles with *Plasmodium* parasites developing inside the hepatocyte and the role of Cullin 3 in endosome maturation, in this thesis, we proposed to characterized the role of Cullin 3 during *Plasmodium* intra-hepatic development using functional assays of gain- and loss- of function, namely by over-expressing Cullin 3 and blocking Cullin 3 signaling using a neddylation inhibitor MLN4924 or depleting Cullin 3, using siRNA. Although gain-of-function experiments and the treatment with neddylation inhibitor MLN4924 were inconclusive, our results showed that Cullin 3 is apparently relevant in the context of malaria infection. In fact, depletion of Cullin 3 expression by siRNA reduced *Plasmodium* levels in Huh7 cells, suggesting that Cullin 3 signaling is important during liver-stage infection. However, more studies are necessary to confirm this phenotype and elucidate the molecular mechanisms behind it.

Keywords: Malaria; Cullin 3; endocytic pathway; liver stage; *Plasmodium* infection.

ABBREVIATIONS

WHO: World Health Organization

RBC: Red blood cell

PV/ PVM: Parasitophorous vacuole; PV membrane

EEF: Exo-erythrocytic form

Ub: Ubiquitin

E3: E3-Ubiquitin ligase

CRL: Cullin-RING ligase

SCF: Skp1-Cullin-F box proteins

Cul: Cullin

BTB: Brac/tramtrack/broad-complex

BCR: BTB-Cul3-Rbx1

MLN4924: NAE inhibitor

NAE: NEDD8 activating enzyme

EGFR: Epidermal growth factor receptor

IAV: Influenza A virus

RNAi: RNA interference

ESCRT: Endosomal sorting complex required for transport

Huh7: Human hepatoma cell line

HeLa: Human cervix carcinoma cell line

RPMI: Roswell Park Memorial Institute medium

DMEM: Dulbecco's Modified Eagle Medium

HEPES: 4-(2-hydroxyethyl)-1-piperazineethanesulfonic acid

FBS: Fetal bovine serum

RT: Room temperature

GFP: Green fluorescent protein

hpi: Hours post-infection

hpt: Hours post-transfection

DMSO: Dimethyl sulfoxide

qRT-PCR: Quantitative real-time reverse transcription polymerase chain reaction

siRNA: Short interfering RNA

HPRT: Hypoxanthine guanine phosphoribosyltransferase

FACS: Fluorescence-activated cell sorting

PBS: Phosphate-buffered saline

PFA: Paraformaldehyde

SDS-PAGE: Sodium dodecyl sulfate polyacrylamide gel electrophoresis

BSA: Bovine serum albumin

TCL: Total cellular lysate

Tub: γ-Tubulin

TABLE OF CONTENTS

1. INTRODUCTION

1.1. Etiology of Malaria infection

Malaria is a parasitic disease that has been a primary concern to humanity for centuries, and continues to be a leading cause of illness and death globally. It is estimated that 3.4 billion people around the world (one half of the world's population) is at risk of malaria and 219 million cases are estimated to have occurred. Only in sub-Saharan Africa the disease kills approximately 660,000 people annually, mostly children under five years of age, resulting in a child's death in every 40 seconds (World-Health-Organization, 2013). Despite global economic development more people die from malaria nowadays than 40 years ago, being considered the fifth leading cause of death in low-income countries (Sachs and Malaney, 2002).

Malaria can be caused by five species of intracellular protozoan parasite that affect humans, and all of these species belong to the genus *Plasmodium*: *P. falciparum*, *P. vivax*, *P. ovale*, *P. malariae* and *P. knowlesi*. Of these, *P. falciparum* and *P. vivax* are the most deadly species and causative of severe disease (cerebral malaria, severe malarial anemia, placental malaria or acute lung injury)(Guerin *et al.*, 2002). High mortality rates due to malaria are localized in tropical regions such as Sub- Saharan Africa, South East Asia, and around the Amazon rainforest in South America, as shown in Figure 1.

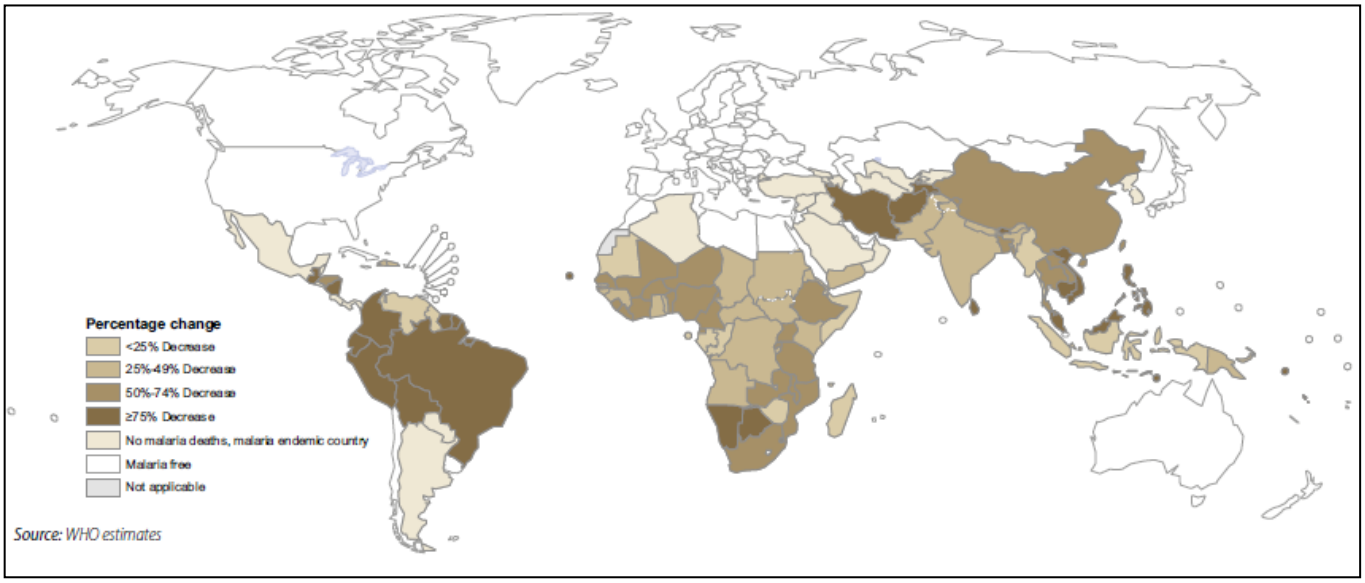

Figure 1: Malaria mortality rates (percentage change between at 2000-2012). Tropical and subtropical regions are affected by malaria worldwide (adapted from WHO world malaria report, 2013).

The impact of malaria is immense and extends far beyond measurement of mortality and morbidity. Besides its social impact malaria has health costs and obvious economic consequences, contributes to prevent social and economic growth in already impoverished

countries (Gallup and Sachs 2001). Currently, the fight against malaria is focused on mosquito eradication, reduction of human–vector contact and disease prevention and treatment using antimalarial drugs. A viable vaccine is not yet available, despite the significant efforts that have been made to develop one. Drug therapy, a key part in malaria control, faces increased resistance worldwide, with no drug being universally effective, and so malaria continues to be a threatening global health problem (Greenwood *et al.*, 2005).

1.2. Parasite and life cycle

Malaria is caused by *Plasmodium*, an apicomplexan parasite transmitted to the vertebrate host through the bite of an infected female *Anopheles* mosquito. There are about 400 different species of *Anopheles* mosquitoes, but only 30 of these are vectors of major importance in transmitting malaria, with the most common and efficient vector species being *Anopheles gambiae, Anopheles arabiensis, Anopheles funestus, Anopheles nili* and *Anopheles moucheti* (Fontenille and Simard, 2004). Because of disparities in eco-systems across regions, differences may exist in the type of species that are predominant in transmitting the disease in different locations (Tanga *et al.*, 2010).

Apicomplexa are unicellular eukaryotes which are obligatory intracellular parasites with short-lived extracellular stages. Unlike many other microbial organisms which utilize phagocytic properties of their host cells for invasion, apicomplexa invasion involves a specialized organelle particular to these parasites, the apicoplast. *Plasmodium* parasites have a complex life-cycle, consisting of the asexual stages, in the vertebrate host, and the sexual stages that take place in the mosquito vector. The infection in vertebrates starts when the mosquito injects *Plasmodium* sporozoites into the skin (Figure 2). After traversing the dermis the parasites enter the circulatory system and travel to the liver where they will complete the *silent* phase of their development (Matsuoka *et al.* 2002; Amino *et al.* 2006). In the liver, sporozoites migrate through several hepatocytes before establishing infection in one cell (Mota *et al.*, 2001). The *invasion* of the final hepatocyte is done by inducing the invagination of the host cell membrane, resulting in the formation of a parasitophorous vacuole (PV) surrounded by a host cell-derived membrane (the parasitophorous vacuole membrane, PVM). This asymptomatic developmental step will eventually lead to the release of thousands of new parasites, called merozoites, into the bloodstream, initiating the symptomatic stage of the disease (Mota *et al.* 2001; van de Sand *et al.* 2005). The merozoites then invade red blood cells (RBCs) and mature into schizonts. Within the blood stages, merozoites either undergo repeated cycles of multiplication or transform into gametocytes, which are taken up by a female *Anopheles* mosquito. Within the mosquito, the parasite undergoes further transformation and the sexual replication takes place. After

approximately two weeks the mosquito becomes infectious for humans and the cycle repeats itself (Warrell and Gilles 2002).

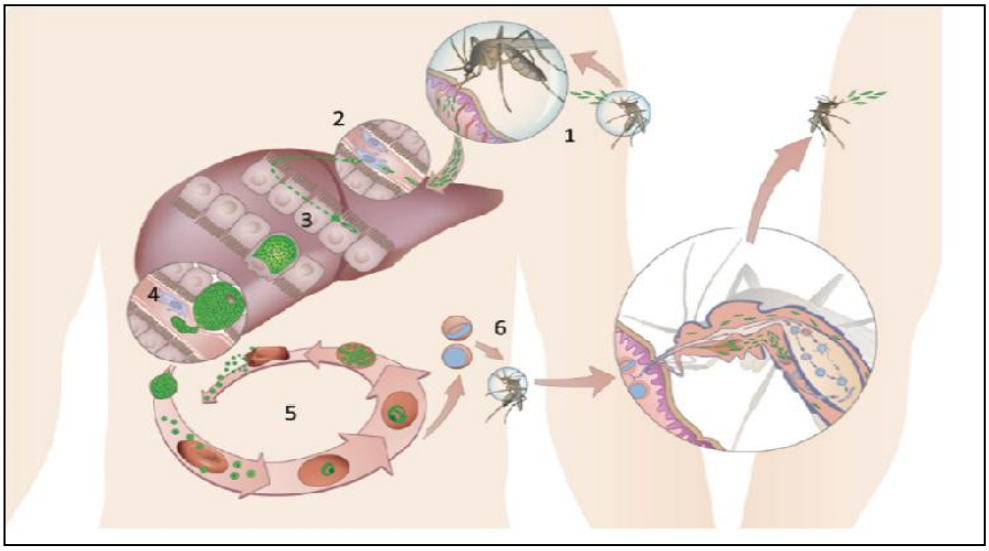

Figure 2: *Plasmodium spp.* life cycle. (1) During a blood meal of a female *Anopheles* mosquito, sporozoites contained in the salivary glands are injected into the dermis of a vertebrate host. The sporozoites enter the bloodstream and travel to the liver (2) where they will traverse a few hepatocytes before invading a final one (3). The parasite will grow and replicate into thousands of merozoites that will be released into the blood stream (4) initiating the blood stage cycles of asexual replication inside RBC (5). Some merozoites can develop as gametocytes that can be ingested by another female *Anopheles* mosquito through blood meal (6), leading to a new cycle of infection (adapted from (Prudêncio and Mota, 2007).

Although the clinical symptoms only appear during the erythrocytic stage of *Plasmodium's* life cycle it should not be disregarded that the asymptomatically pre-erythrocytic stage (also referred to as liver stage) is essential for the malaria infection outcome. However, many aspects of parasite development inside the liver cell are still poorly understood, mainly due to the relative inaccessibility and low abundance of these stages for detailed cellular and molecular studies (Kappe and Duffy, 2006). Also, large and detailed studies of liver stage development are difficult due to the prerequisite of freshly extracted infectious sporozoites (breeding of infectious mosquitoes is a necessity) and to the low infection rates obtained *in vitro* (Prudêncio and Mota, 2007) and *in vivo* (Heussler and Doerig, 2006). Despite these restrictions, malaria researchers have been working towards an understanding of the biology behind the malaria liver stage and, during this journey, huge steps have been made to disclose the processes involved in this stage. A significant amount of *in vitro* and *in vivo* research has been conducted on this stage by taking advantage of model rodent malaria parasites, such as *P. berghei* and *P. yoelii* (Prudêncio, Rodriguez, and Mota 2006; Bano *et*

al. 2007). These models are analogous to human and primate parasites in terms of biology, physiology and life cycle (Sherman, 1998). Furthermore, these parasites are not dangerous to humans representing good models for experimental studies of mammalian malaria (Sherman, 1998). The availability of transgenic rodent *Plasmodium* parasites that express fluorescent or luminescent reporter proteins (Franke-Fayard *et al.* 2004; Frevert *et al.* 2005) has provided novel opportunities to examine in real time the development of liver stages, both in cultures of isolated hepatocytes or hepatoma cell lines and in laboratory animals (Amino *et al.*, 2006).

1.3. Endocytic pathway during *Plasmodium* liver infection

The invasion of hepatocytes by malaria sporozoites is characterized by the formation of a Parasitophorous Vacuole Membrane (PVM), a process involving partial invagination of the host cell plasma membrane, although the molecular players involved in PVM formation and maintenance remain largely unknown (Mota *et al.*, 2001). Once this specialized intracellular niche is established, parasite replication and growth may commence. Dramatic morphological as well as gene expression modifications occur at this stage and the parasites achieve one of the highest replication rates known within eukaryotic species (Sturm *et al.* 2006; Albuquerque *et al.* 2009; Stanway *et al.* 2011). In humans, the hepatic stage of the infection lasts 6-10 days during which the number of parasites expands enormously, up to 40,000 fold. This high multiplication rate imposes a significant demand of nutrients and therefore it is likely that *Plasmodium* has developed mechanisms to exploit the host cell resources. Key to an intracellular lifestyle is the ability to interact with the host endomembrane system to uptake nutrients and/or avoid pathogen degradation. As such, intracellular pathogens have evolved a variety of mechanisms to achieve this, for example, by blocking fusion with the lysosomes, as is the case with *Salmonella*, *Mycobacterium* and *Legionella* species (Méresse *et al.* 1999; Vergne *et al.* 2005; Isberg, O'Connor, and Heidtman 2009). The endomembrane system is comprised of the different organelles of the secretory and endocytic pathways that are suspended in the cytoplasm of eukaryotic cells. The endomembrane system includes: the nuclear envelope, the endoplasmic reticulum, the Golgi apparatus, lysosomes, vacuoles, vesicles, endosomes and the cell membrane. The endocytic pathway starts with endocytosis forming a vesicle. The endocytosed cargo is usually delivered to the early endosome where sorting occurs. Cargo-specific sorting leads to distinct subsequent cargo itineraries. Cargo can be routed from the early endosome to late endosomes and lysosomes for degradation; to the trans-Golgi network (TGN); or to recycling endosomal carriers that bring the cargo back to the plasma membrane (Grant and Donaldson, 2009). Endocytic pathways plays key roles in several biological functions, such as, nutrient uptake, cell signaling, and changes in cell shape (Nebenführ, Ritzenthaler, and

Robinson 2002; Sigismund *et al.* 2008). In the liver, *Plasmodium* parasites develop surrounded by host late endosomes and lysosomes, as show in figure 3. Although no fusion and acidification of the parasitophorous vacuole is observed (Lopes da Silva *et al.*, 2012). These observations suggest that, rather than parasite elimination, host vesicles from the endolysosomal pathway could be important for schizont development, but the mechanism remains elusive.

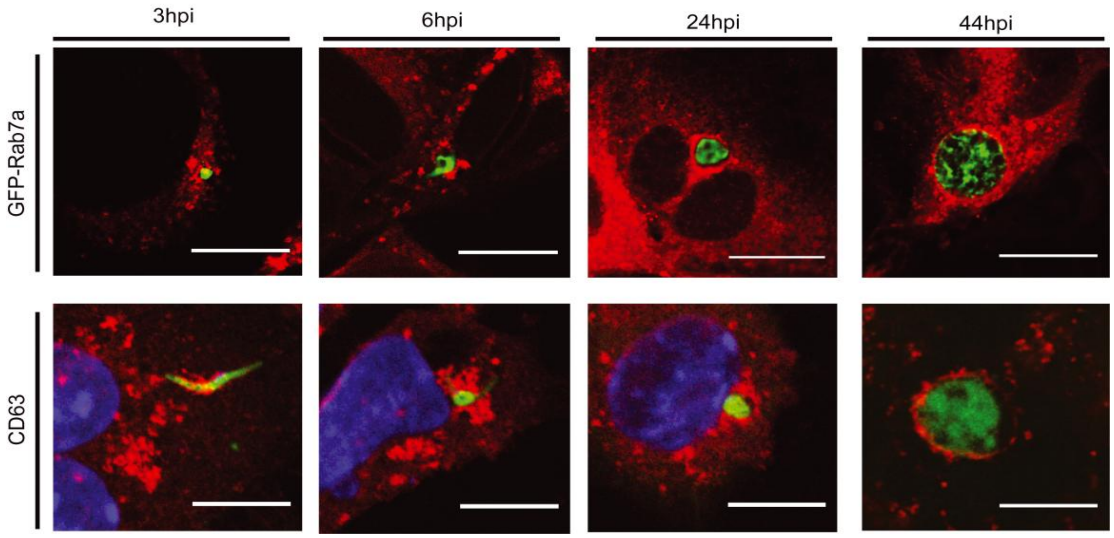

Figure 3: *Plasmodium berghei* parasites develop in liver cells surrounded by vesicles from the host endolysosomal pathway. Hepa1-6 cells were transduced with GFP-Rab7a (red) prior to infection with *P. berghei* sporozoites, fixed at the time-points indicated and subsequently stained with anti-Hsp70 antibody (green). Samples were stained with anti-CD63 (red) and anti-GFP (green) antibodies. (Hpi, hours post-infection. Scale bars: 10 µm; adapted from Lopes da Silva *et al.* 2012).

1.4. Ubiquitination and the Family of Cullin-RING ligases (CRLs)

Ubiquitin system is a post-translational modification that consists in the attachment of an ubiquitin to a substrate protein. The protein modifications can be either a single ubiquitin protein or chains of ubiquitin (Pickart and Eddins, 2004). Ubiquitin system involves three enzymatic components that participate in a cascade of ubiquitin transfer reactions: ubiquitin-activating enzymes (E1), ubiquitin-conjugating enzymes (E2), and ubiquitin ligases (E3) (Mukhopadhyay and Riezman, 2007). Ubiquitination is a major player regulating many biological processes, such as protein trafficking, DNA repair, protein–protein interactions, and proteolysis (Hershko and Ciechanover 1998; Pines and Lindon 2005). The last step of ubiquitin conjugation is controlled by E3 ubiquitin ligase, which is responsible for the specific recognition of the substrates of the ubiquitin system. One prominent collection of E3 enzymes are the Cullin-RING ligases (CRLs). CRLs are multimeric protein complexes composed of a Cullin scaffold that bridges a C-terminal domain (CTD)-bound, RING E3

enzyme, and an N-terminal domain (NTD)-interacting substrate adaptor module. CRLs play a role in diverse cellular processes, including multiple aspects of the cell cycle, transcription, signal transduction, and cell growth, among others (Petroski and Deshaies 2005; Lu and Pfeffer 2013). This diversity of functions is given by each of the adapters present in the complex. The Cullin family is highly conserved among species; six different Cullins proteins have been identified in mammals (Cullin 1, Cullin 2, Cullin 3, Cullin 4a, Cullin 4b and Cullin 5), each Cullin forms a distinct class of CRLs consisting of different adapters and/or substrate recognition subunits (Marín, 2009). The activity of CRLs is regulated by the reversible conjugation of a small ubiquitin-type protein, with highly conserved 81-residues, known as Neural precursor cell Expressed Developmentally Down-regulated protein 8 (NEDD8), a process called neddylation (figure 4) (Wimuttisuk and Singer 2007; Bennett *et al.* 2010). This activation process is essential for the association of the CRL with the E2 enzyme, delivering the ubiquitin moiety to the target proteins (Wu *et al.* 2005).

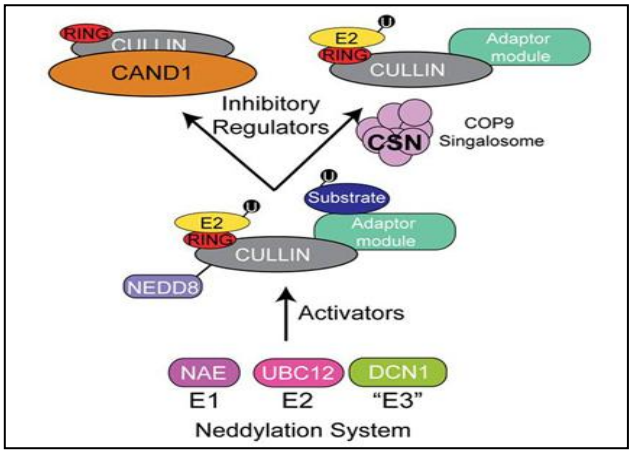

Figure 4: Regulatory mechanisms governing Cullin-Ring ligase activity (adapted from Bennett *et al.* 2010).

1.5. Regulation and maturation of endocytic pathway by Cullin 3

The Cullin 3 forms a catalytically inactive BTB-Cul3-Rbx1 (BCR) ubiquitin ligase. Compared to other Cullin-based complexes, the Cullin 3 is quirky: it does not require different adapters in order to recognize its target protein, but only requires a protein with a bric-a-brac/tramtrack/broad-complex (BTB) domain for recognizing activity (Andérica-Romero *et al.*, 2013). It has been shown that Cullin 3 is specifically activated (neddylated) at the plasma membrane and found associated with vesicular markers for intracellular trafficking (Hubner and Peter, 2012). In addition, Cullin 3-mediated ubiquitilation has recently emerged as a potencial regulator involved the endolysosomal pathway, in particular secretion and endosome maturation (Huotari *et al.*, 2012). Depletion of Cullin 3 by RNA interference (RNAi)

affects intracellular trafficking of two well-studied cargos—the influenza A virus (IAV) and the epidermal growth factor receptor (EGFR). Upon Cullin 3-depletion, infection of IAV decreases dramatically. Cullin 3-mediated ubiquitylation appears to be needed for IAV penetration from late endosomes and/or subsequent viral uncoating. Moreover, EGFR degradation is significantly delayed in Cullin 3-depleted cells that also resulted in the deformation late endosome and lysosome morphology (Huotari *et al.*, 2012). However, the BTB domain-substrate receptors involved in Cullin 3 endosomal transport remains unidentified (Stogios *et al.* 2005; Schnatwinkel *et al.* 2004). The endocytic pathway is regulated at different levels by ubiquitination. The covalent attachment of one, or more, ubiquitin moieties to a certain membrane receptor may regulate the entry in the pathway, the recycling of the receptor or its degradation in the lysosome (Chen and Sun, 2009). The dissection of the molecular and functional mechanisms underlying the endocytic pathway is central for the understanding of many physiological and disease processes (Sigismund *et al.*, 2008).

2. Aims

Given the important association of the host endocytic pathway vesicles with developing *Plasmodium* parasites in the hepatocyte and the role of Cullin 3 in regulation and endosome maturation, the main goal of this project was to evaluate the role of Cullin 3 during *Plasmodium* intra-hepatic development. Using the rodent model *Plasmodium berghei* we aimed at:

I. Analyze the effect of over-expressing Cullin 3 on parasite development;

II. Block Cullin 3 signaling in hepatocytes, using a neddylation inhibitor and/or depleting Cullin 3 using siRNA, and access the effect on *Plasmodium* development and association with endo-lysosomes.

3. Materials and Methods

3.1. Culture of human cell-lines

Two cell-lines were used: the human hepatoma cell line (Huh7) and the human cervix carcinoma cell line (HeLa). Huh7 cells were cultured in RPMI-1640 supplemented with 10% heat-activated Fetal Bovine Serum (FBS), 1% penicillin/streptomycin solution, 1% L-Glutamine, 1% Non Essential Amino Acids and HEPES buffer (all from Gibco/Invitrogen). HeLa cells were cultured in Dulbecco's Modified Eagle Medium (DMEM) supplemented with 10% FBS, 1% penicillin/streptomycin solution, 1% L-Glutamine, 1% Non Essential Amino Acids and 1% HEPES (all from Gibco/Invitrogen). Cells were cultured in petri dishes or flat bottom plates of 6, 24 or 96 wells and incubated at 37ºC with 5% CO_2. Culture medium was changed every 48 hours. For experimental setups, cells were detached with trypsin solution for 5 min at 37°C. The action of trypsin was stopped by resuspending the cells in an appropriate volume of complete medium. Cells were recovered by centrifugation at 1.200 revolutions per minutes (rpm) for 5 minutes, room temperature in a bench top centrifuge with a swing out rotor (Eppendorf centrifuge 5810R). Cells were counted by microscopy using a Neubauer chamber. An appropriate number of cells was seeded in appropriate dishes/plates and further incubated in a 5% CO2, 37°C incubator.

3.2. *Plasmodium berghei* transgenic-line

For this study was used the transgenic Green Fluorescent Protein (GFP) – expressing *P. berghei* ANKA (*Pb*GFP, parasite line 260 cL2; Franke-Fayard *et al.*, 2004). *Anopheles stephensi* mosquitoes that had blood a meal from mice infected with GFP - *P. berghei* parasites were housed in appropriate cages in humidified incubators, in compliance with the guidelines from the Ethics Committee of the Institute. At about day 24 post-feeding, *P. berghei*-infected salivary glands were dissected from infected mosquitoes into an appropriate volume of DMEM medium in a 1.5 ml microtube. Then they were smashed and passed through a cell strainer. The number of sporozoites from each dissection were counted using a Neubauer chamber previously placed in a humidity chamber for 10 min, by calculating the average of sporozoites per quadrant x 10^4 x dilution factor x volume.

3.3. Infection with *Plasmodium berghei* sporozoites

Infections were performed with freshly dissected *Plasmodium berghei* sporozoites, resuspended in an appropriate volume of RPMI-1640 or DMEM complete medium supplemented with 0,02% Fungizone. For each experiment, the determined amounts of sporozoites were added to cells that were then centrifuged at 3000 rpm for 5 min, at room

temperature. Cultures were incubated at 37°C, 5% CO_2 for the appropriate period of time. Culture medium, supplemented with 0.02% Fungizone, was changed every 24 hours.

3.4. Over-expression of Cullin 3

Reverse transfection of HeLa cells was performed using GeneJuice Transfection Reagent (Novagen), following the manufacturer's instructions. Briefly, for 6-well plate transfection experiments, 3 µl of GeneJuice were mixed with 100 µl serum-free medium into a sterile tube in separate wells and incubated for 5 min at room temperature. For each well, 2 µg of plasmidic DNA were added to the GeneJuice Transfection Reagent/serum-free medium mixture. The GeneJuice Transfection Reagent/DNA mixture was incubated for 15 min at room temperature and then added to the freshly trypsinized HeLa cells. This was followed by the addition of 300000 HeLa cells per well in DMEM supplemented with 10% FBS, 1% penicillin/Streptomycin solution, 1% L-Glutamine, 1% Non-Essential Amino Acids and 1% HEPES, the medium was changed at 24h post-transfection. For 24-well plate transfection experiments, 1.5 µl of GeneJuice were mixed with 25 µl serum-free medium into a sterile tube in separate wells and incubated for 5 min at RT. For each well 0.5 µg of plasmidic DNA were added to the GeneJuice Transfection Reagent/serum-free medium mixture. The GeneJuice Transfection Reagent/DNA mixture was incubated for 15 min at room temperature and then added to the freshly trypsinized HeLa cells. This was followed by the addition of 50000 HeLa cells per well in DMEM supplemented with 10% FBS, 1% penicillin/Streptomycin solution, 1% L-Glutamine, 1% Non-Essential Amino Acids and 1% HEPES, the medium was changed at 24h post-transfection. The cells were incubated for 30 hours and infected with *P. berghei* sporozoites as previously described.

3.5. Inhibition of CRLs activation through neddylation inibition

MLN4924, inhibitor of NEDD8-activating enzyme (Millennium Pharmaceutics, Inc.; Soucy *et al.*, 2009) was resuspended in Dimethyl Sulfoxide (DMSO) in a stock concentration of 30 mM. The final concentration used of MLN4924 was obtained by diluting the stock in complete medium. MLN4924 was added to the cells 24h before-infection. Technical duplicates were done for each condition and DMSO was used as a control.

3.6. Knockdow of Cullin 3 with siRNA

Cells were transfected with target specific or scramble siRNA sequences purchased from Ambion. According to the manufacturer's instructions, 5 nM powder of oligonucleotide sequence was re-constituted with 100 µl of Nuclease-free RNase-free H_2O to obtain 50 µM stock solutions. Stocks were stored at -80◦C. A working concentration of 2 µM was prepared

from a 50 µM stock solution by adding an appropriate amount of Nuclease-free RNase-free H_2O. For 96-well plate transfection experiments, 1.5 µl of target specific or control siRNA was pre-diluted with 8.5 µl of OptiMEM in separate wells. This was followed by the addition of 10 µl of a pre-diluted mix of Lipofectamine RNAi MAX in OptiMEM. To every 9.8 µl of OptiMEM, 0.2 µl of Lipofectamine RNAiMAX was added and mixed before being added to the siRNAOptiMEM mix. The 1:1 siRNA pre-dilution and Lipofectamine RNAi MAX pre-dilution were mixed well and incubated for 20 min at room temperature. The 20 µl of siRNA/Lipofectamine complex was transferred per well to a new 96-well plate for cell culture. This was followed by the addition of 6000 cells per well in a final volume of 100 µl of DMEM supplemented with 10% FBS, 1% L-Glutamine, 1% Non-Essential Amino Acids and 1% HEPES without antibiotics. Unused edge wells were filled with H_2O or PBS and the cells were incubated at 37ºC, 5% CO_2. For 24-well plate, 7.5 µl of target specific or control siRNA was prediluted with 42.5 µl of OptiMEM and mixed in 1:1 ratio with a Lipofectamine RNAi MAXOptiMEM mix that was prepared by pre-diluting 1 µl of Lipofectamine RNAi MAX with 49 µl of OptiMEM. The siRNA/Lipofetamine mix was transferred to a new 24-well plate and 40000 cells were added in 400 µl of DMEM complete medium without penincillin/streptomycin. Cells were incubated for 36 hours and infected with *P. berghei* sporozoites as previously described.

3.7. Flow cytometry analysis

Flow cytometry analysis was done for the *in vitro* infections with the GFP-expressing *Plasmodium berghei* parasite line, *Pb*GFP, as previously established (Prudêncio *et al.*, 2008). This technique offers the possibility of further dissecting the infection process in terms of percentage of cells invaded and intracellular development of the parasite. Based on the experimental design, cells that had been previously seeded in 24-well plates were infected with 40000 GFP-expressing *P. berghei* sporozoites in the presence of 0.02% fungizone. The plates were further incubated for 5h, 24h or 48h. In order to assess percentage of invasion, infection was stopped at 5 hours post-infection. The culture medium was removed and cells were rinsed twice with PBS. An appropriate volume of 0.05% trypsin was added to cells and incubated for 5 min at 37◦C. Cells were re-suspended in an appropriate volume of 10% FBS-supplemented PBS in order to inhibit the action of trypsin. Cells were centrifuged for 5 min at 2000 rpm. Supernatant was removed and cells were re-suspended in about 250 µl of 2% FBS-supplemented PBS for analysis using the Blue Laser (488 nm) and appropriate gating of cells (see gating strategy in Appendix II).

3.8. Immunofluorescence

For intracellular localization of *Plasmodium berghei* in Huh7 cells or HeLa cells by immunofluorescence, *Plasmodium berghei* infected cells were seeded on glass coverslips on 24-well plates, previously transfected with siRNA or subjected to drug treatments**.** At the appropriate time-points cells were washed with PBS, and fixed with 4% paraformaldehyde (PFA) for 15 min at room temperature. Cells were then washed twice with PBS and incubated 10 min at room temperature with permeabilization solution (PBS 1X with 0.1% Triton X or 0.1 % saponin). Cells were washed twice with PBS for 10 min. The blocking step was performed in blocking solution (PBS 1X with 1% bovine serum albumin) for 30 min at room temperature. Cells were incubated with primary antibodies in blocking solution for 1h in a humid chamber. After three washs in PBS, samples were incubated with secondary antibodies in blocking solution for 45 min in a humid chamber and washed again three times with PBS. The mounting step was performed using Fluoromount G solution. Slides were allowed to dry in a dark place. The list of antibodies and dilutions used are listed in Appendix I, table 3.

Confocal images were acquired using LSM 510 META confocal microscope with the following parameters: excitation at 405 nm, Band Pass (BP): 420 nm-480 nm, excitation at 488 nm, BP: 505 nm-530 nm, excitation at 594 nm: Long Pass (LP): 615 nm. Images were processed with Image J software.

3.9. Western blots

Western blots were done with MiniProtean Tetra Cell equipment (BioRad). 1.5 mm Tris-glycine SDS-PAGE resolving and stacking gels were prepared at 10%. Gels were loaded with 40 µg of samples and 7 µl of molecular weight marker (Precision Plus Protein™ Dual Color Standards - BioRad or ColorBurst™ Electrophoresis Marker - Sigma). Running buffer was prepared with Tris, Glycine, SDS and H_2O. Gels were run at constant voltage of 120 V until samples entered the resolving gel and then voltage was increased to 180 V. Transfer to nitrocellulose membrane was performed using iBlot® Dry Blotting System (Life Technologies) for 7 min 30 sec. Blocking of nitrocellulose membrane was done in a 5% BSA solution in TBST 0.1% (blocking solution). Membrane was incubated in blocking solution during 1h at room temperature with slow agitation. Primary antibody incubation was done overnight at 4ºC in slow agitation. Nitrocellulose membranes were washed three times in TBST 0.1% with rapid agitation during 10 min at room temperature. Secondary antibody incubation was done at room temperature during 1h with slow agitation, followed by three washes with TBST 0.1% with rapid agitation during 10 min at room temperature. Detection of

the immunoblot was done by incubating the membranes 1 min in the dark with detection solution (Supersignal West pico chemiluminescent substrate HRP – ThermoScientific) and proceeding to the exposure and developing of films (Fuji medical X-ray film, Fujifilm).

3.10. RNA extraction and quantification

RNA was extracted from cells using High Pure RNA Isolation kit (Roche) or Trizol Reagent (Invitrogen) according to the manufacturers´ instruction. With High Pure RNA isolation kit, cells were rinsed briefly with RNase-free PBS and resuspended in two-third volume of lysis/-binding buffer and one-third volume of PBS. The sample was transferred to a High Pure filter tube and inserted in a collection tube. The samples were centrifuged for 15 sec at 8000 x g. The flow-through liquid was discarded and the High Pure Filter tube was re-inserted in the collection tube. One hundred microlitres of DNase I in DNase incubation buffer was added to each Filter tube and incubated for 15minutes at room temperature. The column was washed once with 500 µl of Wash Buffer I by centrifuging at 8000 x g for 15 sec and twice with 500 µl and 200 µl of Wash Buffer II by centrifuging at 8000 x g for 15 sec and 2 min respectively. The RNA was eluted with an appropriate volume of Elution Buffer by centrifuging at 8000 x g for 1 min. To isolate RNA using Trizol reagent, cells were homogenized with an appropriate volume of Trizol reagent and incubated for 5 min at room temperature to allow the complete dissociation of nucleoproteins. An appropriate volume of chloroform was added to the homogenate and the tubes were shaken vigorously with hand for 15 sec. For every ml of Trizol used, 0.2 ml of chloroform was added. The Trizol-chloroform mixture was incubated for 2-3 minutes at room temperature and centrifuged at 13000 rpm for 15 min at 4 ºC. The resultant colorless upper aqueous phase was transferred to a fresh microtube. In order to precipitate the RNA from the aqueous phase, an appropriate volume of isopropanol was added, mixed thoroughly, incubated for 10 min at room temperature, and centrifuged for 10 min at 13000 rpm at 4 ºC. For every ml of Trizol, 0.5 ml of isopropanol was used for RNA precipitation. The supernatant was removed and the pellet was mixed with 1 ml of 75% ethanol, vortexed and centrifuged at 7500 x g for 5 minutes at 4ºC. The supernatant was removed and the pellet was redissolved in an appropriate volume of RNase-free water and incubated at 55-60ºC for 10 min to inactivate RNase. RNase-free sealable microtubes were used for this purpose. RNA was quantified in a NanoDrop® ND-1000 Spectrophotometer machine using 1 µl of sample.

3.11. cDNA synthesis and quantitative RT-PCR

The synthesis of the cDNA from the RNA templates was synthesized using the AMV Reverse Transcriptase kit Roche cDNA synthesis kit. Briefly, 50 ng of RNA was used in each reaction.

The cDNA synthesis protocol was carried out in a Bio-rad machine as follows: 25ºC for 10 min, 55ºC for 30 min, and 85ºC for 5 min. To determine the levels of gene expression study, reactions of Quantitative real-time reverse transcription polymerase chain reaction (qRT-PCR) using SYBR® Green reagent an intercalating double-stranded DNA were made. The reactions were performed using 50 ng of RNA converted into cDNA (cDNA was diluted appropriately for use containing 2 µl corresponding to 50 ng RNA), for total reaction volume of 20 µl. Thus, the reactions were performed for each well with 0.4 µl of each specific primer (10 µM), forward and reverse, 10 µl mix BioRad, 7,2 µl of milli-Q water sterile RNAse free, 2 µl of cDNA from each sample. The thermocycling conditions were: initial step of 50ºC for 2 min, 95ºC for 10 min, followed by 40 cycles at 95ºC for 15 sec and 60ºC for 1 min, melting stage was done at 95ºC for 15 sec, 60ºC for 1 min, and 95ºC for 30 sec (7500 thermocycler Fast Real-Time PCR System, Applied Biosystems). HPRT primers were used as a house-keeping gene for normalization in all experiments. For each sample, technical duplicates were performed, allowing the detection of possible errors. The dissociation curves were also added at the end of the reactions. Negative controls were used (NTC = no template control, NRT = no reverse transcriptase) to confirm the absence of possible contaminants in the reagents used. The results were analyzed using the software program 7500 - Version 2.0.6. Relative expression of each gene of interest, normalized to the house-keeping gene, in each experimental condition (relative to control) was calculated using the delta-delta Ct method.

The primers used in the study are provided in Appendix I, table 1.

4. RESULTS AND DISCUSSION

The role of Cullin 3 in *Plasmodium* intra-hepatic development and association with endo-lysosomes

There are two stages of malaria infection in mammalian hosts, the first phase occurs in the liver and is clinically silent. The infection starts when the mosquito injects *Plasmodium* sporozoites into the dermis of an individual during a blood meal by an infected female *Anopheline* mosquito. Within a few minutes after deposition, the sporozoites migrate through the dermis, enter the circulatory system and travel to the liver (Amino *et al.* 2006; Matsuoka, Yoshida, Hirai, and Ishii 2002) where they migrate through several hepatocytes before invading a final one (Mota *et al.*, 2001). During intrahepatic development, a single sporozoite undergoes extensive rounds of replication generating tens of thousands of blood stage-infectious merozoites (van de Sand *et al.*, 2005). Studies by Lopes da Silva and colleagues showed that *P. berghei* parasites develop in the liver surrounded by host vesicles, namely late endosomes and lysosomes, although no clear aggregation of early and recycling endosomes was observed (Lopes da Silva *et al.*, 2012). Recent data revealed that Cullin 3 plays important roles in vesicular trafficking, in particular secretion and endosome maturation (Huotari *et al.*, 2012). It has been shown that Cullin 3 is specifically activated by neddylation at the plasma membrane and associates with vesicular markers for intracellular trafficking. In addition, depletion of Cullin 3 results in the deformation of late endosomes and causes defect in the transport of endocytic cargo to lysosomes (Huotari *et al.*, 2012). Given the important association of the host vesicles with the developing *Plasmodium* parasites in the hepatocyte and the role of Cullin 3 in regulation and endosome maturation, in this thesis, we aimed at characterizing the role of Cullin 3 during *Plasmodium* intra-hepatic development. For this, we have performed functional assays of gain- and loss- of function, namely by over-expressing Cullin 3 and blocking Cullin 3 signaling using a neddylation inhibitor MLN4924 or depleting Cullin 3, using siRNA.

4.1. Over-express Cullin 3 and analyze the effect on parasite development

We started by checking whether over-expressing Cullin 3 would have any effect on *Plasmodium* infection, as well as in the accumulation of vesicles around parasite.

We began by evaluating the rate/efficiency of transfection in the human hepatoma cells (Huh7) usually used in our infection setups, and in the HeLa cells. For this we used a plasmid expressing GFP and analyze the level of GFP expression by flow cytometry. The

HeLa cells showed better transfection efficiency (30%) compared with cells Huh7 that showed a transfection rate of 0,77% (Figure 5). Based on these results we choose HeLa cells to proceed for the evaluation of the effects of over-expressing Cullin 3 during *Plasmodium* infection. We transfected HeLa cells with a plasmid expressing Cul3-Myc. 36h after transfection cells were infected with freshly dissected GFP-expressing *P. berghei* sporozoites. The analysis was performed by microscopy. Transfected cells were detected with either an anti-Cul3 or anti-myc antibody and parasites were detected using a PVM marker (anti-UIS4 antibody) (Figure 5).

After the analysis of three independent experiments we could not identify sufficient numbers of cells that were both transfected and infected to be able to draw any conclusions on the effect of Cullin 3 over-expression on *Plasmodium* infection. The reason for this might be the combination of the low transfection rate quantified here (30%) with the extremely low infection rate of HeLa cells by *Plasmodium* (<1%). In order to overcome this difficulty, one possibility for further gain-of-function studies would be to create a cell line stably expressing Cullin 3.

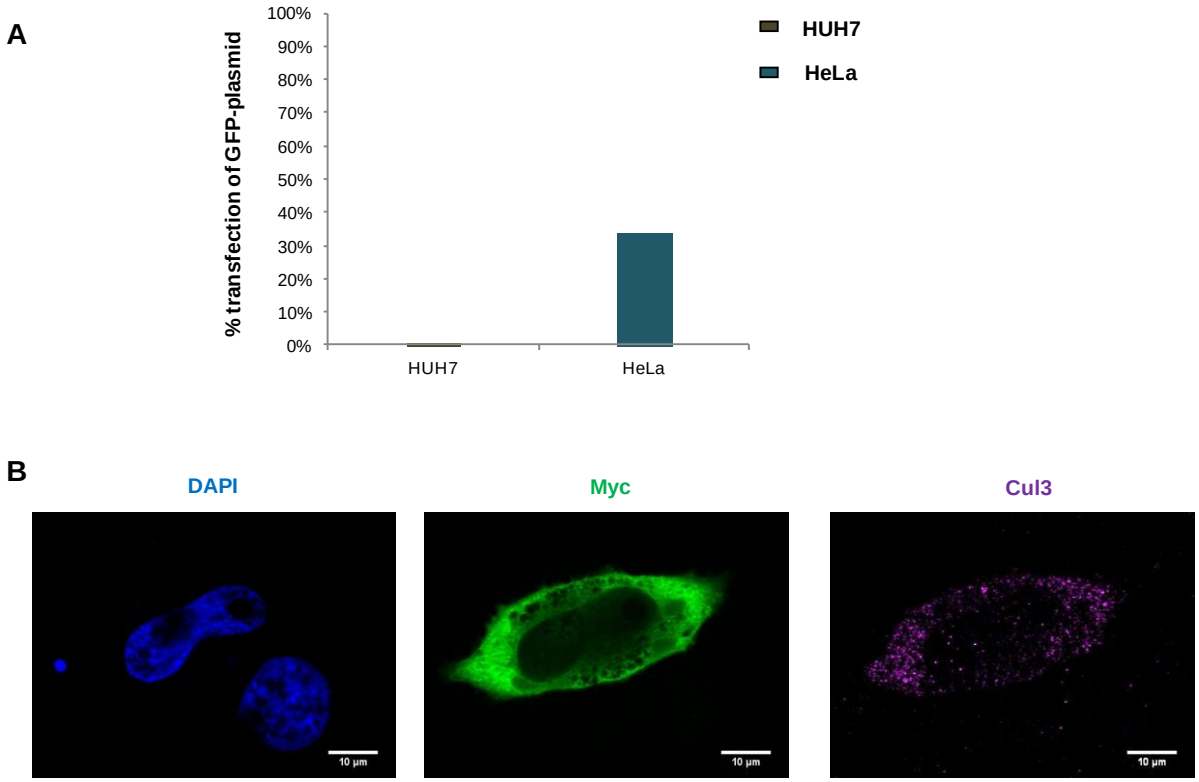

Figure 5: Over-expression of Cullin 3. Huh7 cells and HeLa cells were transfected with pCMV-GFP plasmids and analyzes by flow cytometry at 36 hpt (A). HeLa cells were transfected with pCMV-Cul3-myc plasmids and infected with *P. berghei* sporozoites. Analysis was performed through microscopy. Cells were stained with anti-Myc antibody (green); anti-Cul3 antibody (magenta) and Nuclei were stained with DAPI (blue; B). Scale bars: 10 µm.

4.2. Blocking Cullin 3 signaling, using the neddylation inhibitor MLN4924, in *Plasmodium* liver stage infection

Neddylation, the process of adding the ubiquitin-like molecule NEDD8 to target proteins, is a type of protein post-translational modification. Occurs through the action of a neddylation cascade similar to that used in the ubiquitin system. It involves the successive action of NEDD8-activating enzyme E1 (NAE), NEDD8-conjugating enzyme E2 (Ubc12), and NEDD8-E3 ligase (Xirodimas *et al.*, 2008). Many studies showed that neddylation plays an important role in ubiquitin-mediated proteolysis by modification of Cullins (Soucy *et al.*, 2009). MLN4924 is a newly discovered small molecule inhibitor of NAE (Petroski, 2010). Mechanistically, MLN4924 inhibits NAE activity through the binding to NAE at the active site forming a covalent NEDD8-MLN4924 adduct (Brownell *et al.*, 2010). As a result, Cullin neddylation is blocked leading to CRL/SCF (Cullin-RING-ligases / Skp1-Cullin-F box proteins*)* inactivation and consequently to the accumulation of several key substrates of CRLs. One advantage of MLN4924 is the high specificity toward the CRLs inhibition. In addition, this compound is approved FDA (*Food and Drug Administration*).

We started by confirming the effect the compound MLN4924 in accumulation of autophagosomes vesicles upon blocking Cullin neddylation in our system. The protein microtubule-associated protein light chain 3 (LC3), a mammalian homolog of yeast Atg8, is known to exist on autophagosomes, and therefore, is a widely used marker for autophagosomes (Kabeya *et al.* 2000; Mizushima 2004). Thus, we have performed a microscopy analysis of HeLa cells expressing GFP-LC3 treated with 1 µM the compound MLN4924 during 24 hours, according to what is described in the literature (Lin *et al.* 2010; Zhao *et al.* 2012). We observed that MLN4924 at 1 µM within a period of 24 hours causes accumulation the LC3, and thereby assure the proper functioning of the compound in our hands (Figure 6).

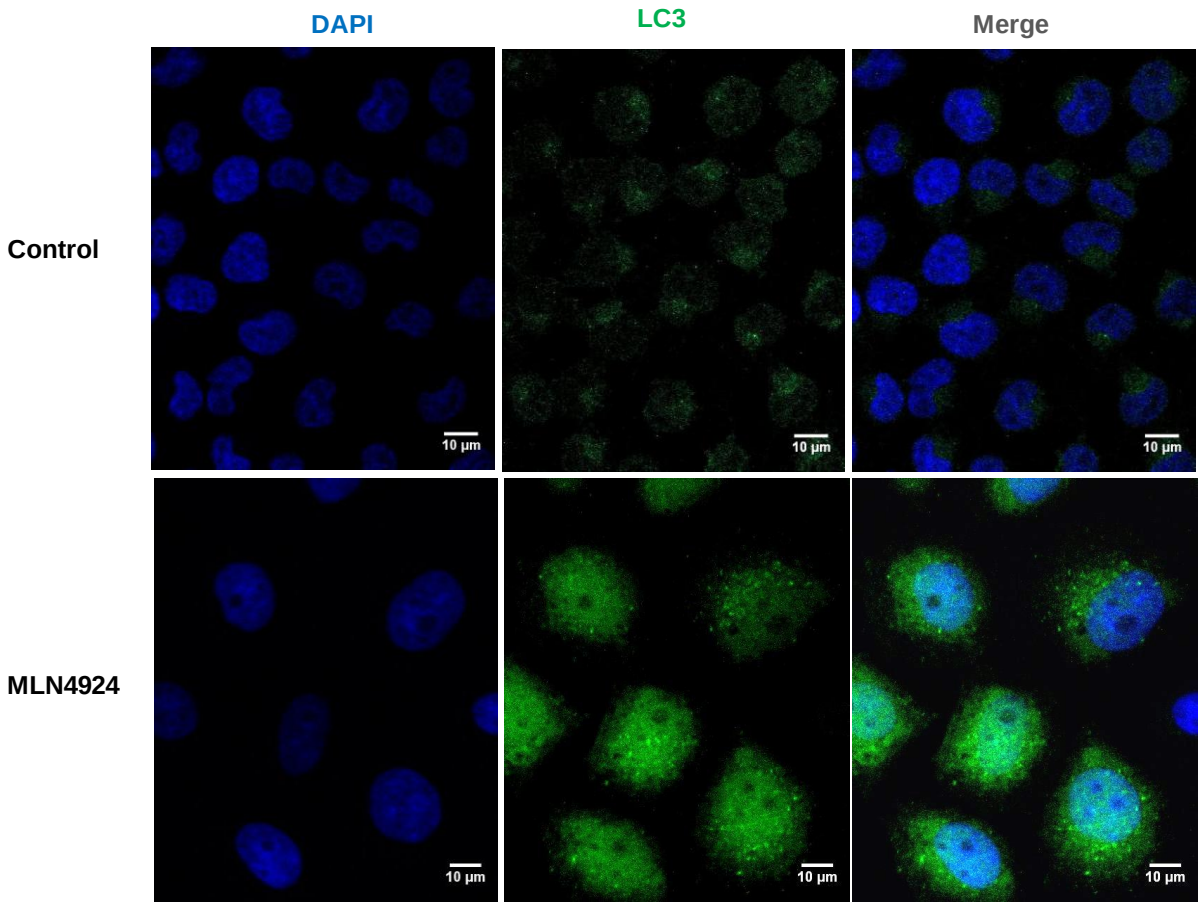

Figure 6: Effects of MLN4924 in the accumulation of LC3 vesicles. Microscopy analysis of HeLa cells expressing GFP-LC3 treated for 24 hours with 1µM MLN4924 or vehicle (DMSO) as control. Staining of vesicles with an anti-LC3 antibody (green) and cell nuclei stained with DAPI (blue). Scale bars: 10 µm.

Next we evaluated the effect of the neddylation inhibitor MLN4924 during *Plasmodium* infection. We first analyzed *Plasmodium* invasion at 5 hpi. We used human hepatoma cells (Huh7) that were infected with freshly dissected *GFP*-expressing *P. berghei* sporozoites. The cells were infected 24 hours after treatment with 1 µM or 10 µM of MLN4924. Control cells were treated with vehicle alone (DMSO) and all the results were normalized to DMSO at 1 µM. Infection parameters were quantified at 5 hpi by flow cytometry. We observed that none of the concentrations significantly affect cell viability (Figure 7A). Similarly, no effect was observed in the levels of *Plasmodium* invasion when cells are treated with MLN4924, as evidenced by the green bars when compared to the control, grey bars (Figure 7B).

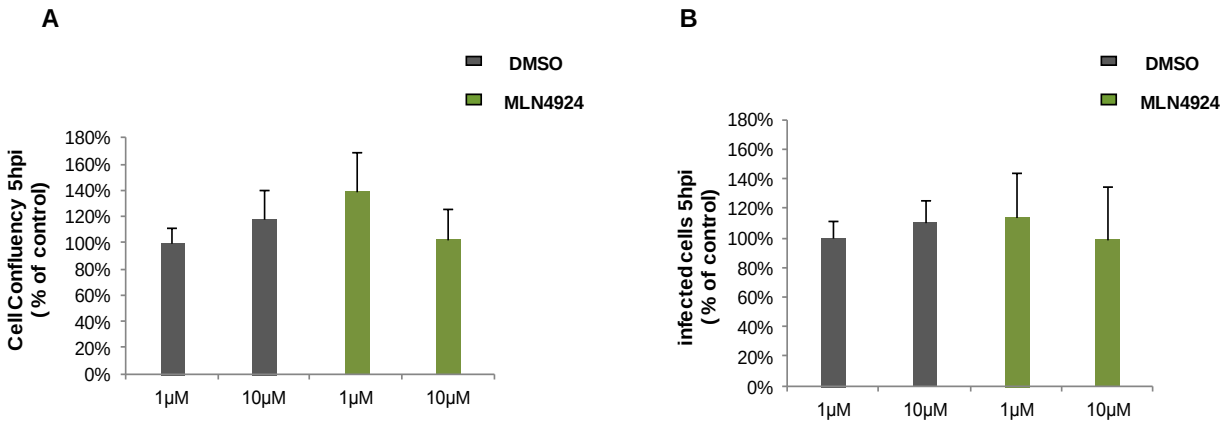

Figure 7: Effect of neddylation inhibition in *Plasmodium berghei* invasion. Flow cytometry analysis of *P. berghei* infected Huh7 cells submitted to treatment with 1 or 10 µM of MLN4924 (green bars) and DMSO (grey bars), The cell confluency (A) and infection levels (B) were determined at 5 hpi and normalized to 1 µM DMSO.

We next evaluated the effect of inhibiting host Cullin 3 signaling using neddylation inhibitor MLN4924 in *Plasmodium* infection levels at 48 hpi. As before, Huh7 cells were infected with *GFP*-expressing *P. berghei* sporozoites 24 hours after the treatment with 1 µM of MLN4924. Control cells were treated with DMSO and all the results were normalized to DMSO. Infection parameters were quantified at 48 hpi by flow cytometry. Our results show that treatment with the lowest concentration of the compound, MLN4924 (1µM) severely interferes with cell numbers (Figure 8A), most likely through the induction of cycle arrest. In addition, the effect on infection levels is only mild, as evidenced by the green bars when compared to the control, grey bars (Figure 8B).

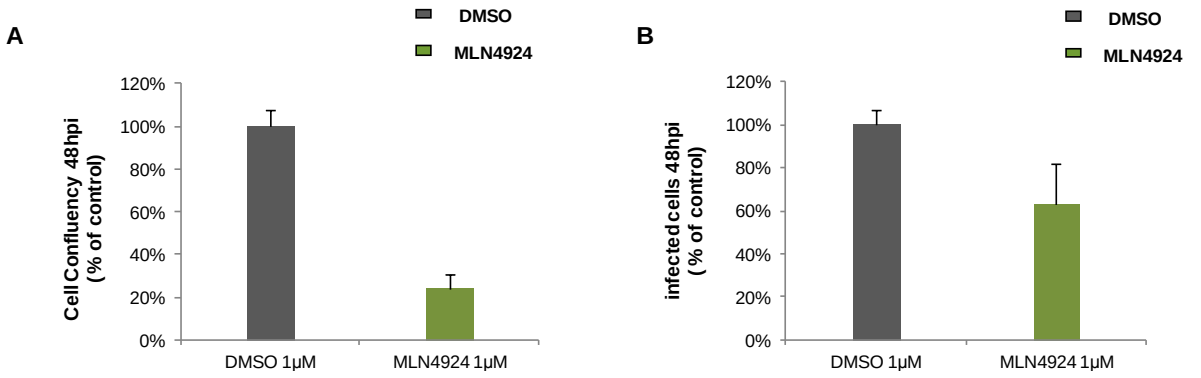

Figure 8: Effect of neddylation inhibition in *Plasmodium berghei* levels of infection at 48 hpi. Flow cytometry analysis of *P. berghei* infected Huh7 cells submitted to treatment with 1 µM MLN4924 (green bars) or DMSO (grey bars). The cell confluency (A) and infection levels (B) were determined and normalized to DMSO.

The effect of MLN4924 on cell growth was further explored aiming to identify any potential cell morphological alterations and eventual indirect effects on *Plasmodium* infection. For this we performed microscopy analysis using Huh7 cells infected with GFP-expressing *P. berghei* sporozoites 24 hours after the treatment with MLN4924 (1 µM). As before, control cells were treated with vehicle alone (DMSO). The results were normalized to DMSO control. Consistently with previous results, when cells were treated with MLN4924 the effect on cell number was observed. We further observe, both by flow cytometry as well as by microscopy, the phenotype of increased cell size, with enormous and irregular nuclei (Figure 9A and 9B), suggesting that indeed the compound is causing cell cycle arrest. Interestingly, although the number of parasites at 48 hpi is not altered (Figure 9C), their size is strongly reduced (Figure 9D and 9E) suggesting that the development of *Plasmodium* parasites upon treatment with the compound is affected.

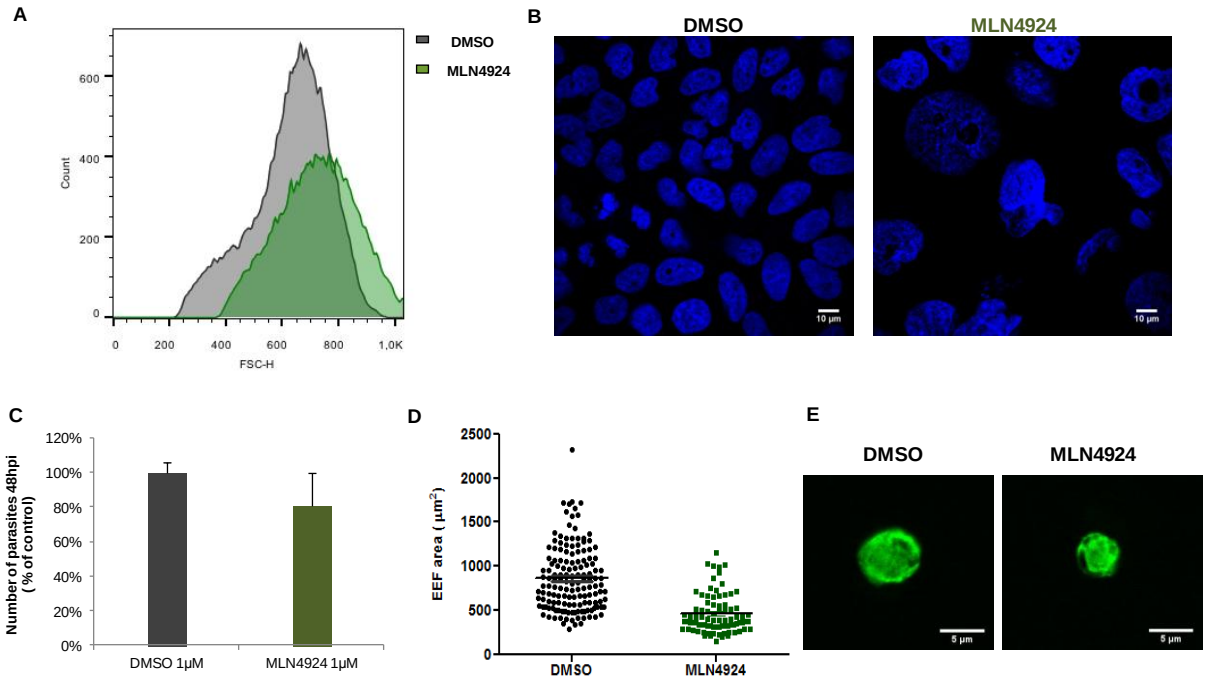

Figure 9: Effect of neddylation inhibition in cell cycle and *Plasmodium berghei* development. Analysis of Huh7cells treated with 1 µM MLN4924 or DMSO showing the differences in cells size upon treatment evidenced by flow cytometry (FSC-histogram) (A) or microscopy analysis (B). In the same experiments, the total number of parasites at 48 hours post-infection was quantified (C) and schizont size was quantified by measuring the area (D). Representative images of parasites at 48 hpi. For microscopy analysis cells were stained with anti-Hsp70 antibody (parasite cytoplasm; green) and nuclei with DAPI (blue).

Overall, our data demonstrate that although there is no significant effect in *Plasmodium* infection levels (Figure 8B and 9C), the development of the parasites is strongly affected upon treatment MLN4924 (Figure 9D). However, treatment with MLN4924 also lead to highly altered morphology in the host cells, which depicted abnormally increased size, enlarged and irregular nuclei (Figure 9B). In fact, these and other effects have been previously described in the literature, mechanistic studies of MLN4924 action in growth suppression of tumor cells revealed that MLN4924 effectively induced apoptosis (Soucy *et al.* 2009; Milhollen *et al.* 2010; Swords *et al.* 2010; Milhollen *et al.* 2011) and senescence (Lin *et al.* 2010; L. Jia, Li, and Sun 2011) in several human cancer cell lines. These observations are associated with DNA damage response, G2 phase arrest; likely triggered by DNA replication due to accumulation of DNA-licensing proteins, resulting from inactivation of CRL/SCF E3 ligase (Luo *et al.* 2012; Blank *et al.* 2013). For these reasons it is not possible to draw any conclusions on the effect of the blocking Cullin 3 signaling in *Plasmodium* infection, through the use of MLN4924.

4.3. SiRNA-mediated knockdown of the host cell Cullin 3

To better evaluate the role of Cullin 3 during liver stage *Plasmodium* infection we used a more specific approach. We used siRNA-mediated knockdown to cause depletion of Cullin 3 in the host cell and evaluate the possible effects on *Plasmodium* infection.

We first assess Cullin 3 mRNA levels after siRNA-mediated Cullin 3 depletion in hepatoma cells. Three different siRNA oligonucleotides targeting human Cullin 3 (named, Cul3#1, Cul3#2 and Cul3#3) were transfected in Huh7 cells. In all experiments, control cells were transfected with a scramble (non-targeting) siRNA oligo (Neg control). Cullin 3 mRNA levels were measured by qRT-PCR at 36 hours and 84 hours post-transfection (Figure 10A and 10B, respectively). The results were normalized as a percentage in relation to the negative control. In order to confirm the decrease also in Cullin 3 protein levels upon depletion, transfected Huh7 cells were also analyzed by western blot 84 hpt. The western blot analysis shows that after knockdown Cullin 3 protein levels are also reduced (Figure 10C; Cullin 3 has a molecular weight of approximately 75KDa).

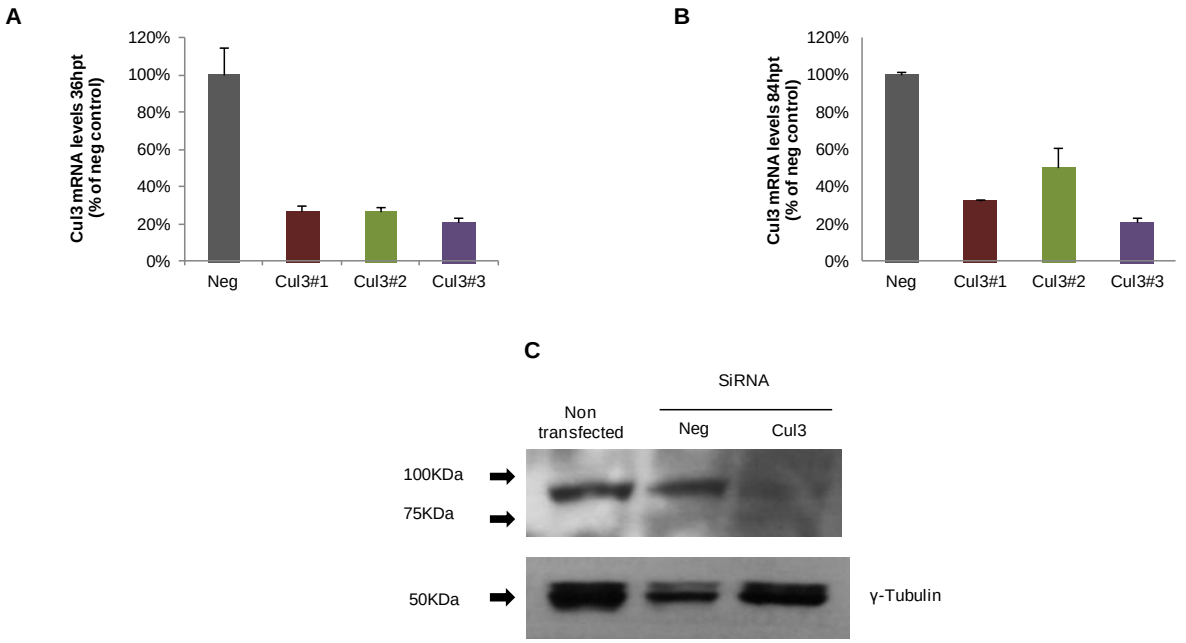

Figure 10: Levels mRNA and protein expression after siRNA-mediated knockdown Cullin 3. Two validated siRNA oligonucleotide targeting human Cullin 3 were reverse-transfected into Huh7 cells and mRNA levels analyzed by qRT-PCR at 36 hours (A) and 84 hours (B) post-transfection. Huh7 cells were transfected with pooled Cullin 3 siRNA oligos or scramble siRNA and subsequently, lysed and immunoblotted with anti-Cul3 and anti-γTubulin (γ-Tub) as loading control (C).

The next step was to evaluate the possible effects of Cullin 3 depletion on *Plasmodium* infection. We choose one oligonucleotide (Cul3#1) to proceed with the analysis; this oligo was chosen based on knockdown efficiency and stability (Figure 10A and 10B). Transfected Huh7 cells were infected with *GFP*-expressing *P. berghei* sporozoites 36 hpt and infection was analyzed by measuring *Pb* 18S rRNA levels by qRT-PCR at 48 hpi. The results suggest that the knockdown of Cullin 3 leads to a decrease in *Plasmodium* infection at 48 hpi (Figure 11A). To check if this effect was due to a decrease in numbers or in parasite development we performed the same experiment but this time analyzed by microscopy, counting the number and measuring the area of the parasites. Parasites were stained using an anti-Hsp70 antibody (parasite cytoplasm). The result of number of the parasites is normalized to Neg control. Consistently, we observed a decrease in *Plasmodium* numbers at 48 hpi upon Cullin 3 knockdown (Figure 11B). However, the parasite development did not showed significant alterations (Figure 11C and 11D).

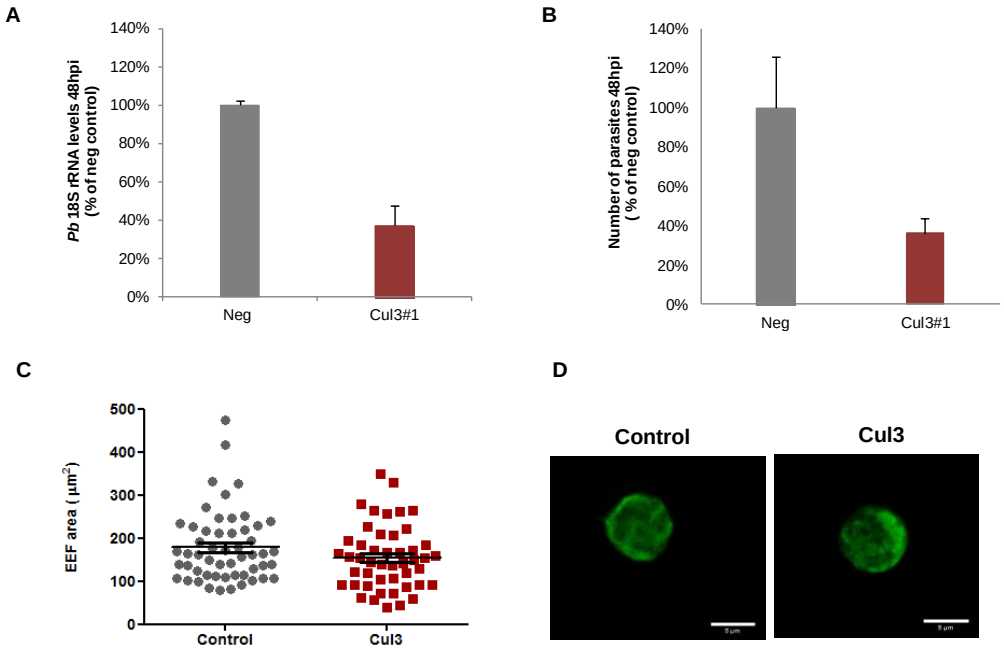

Figure 11: Effect of siRNA-mediated knockdown Cullin 3 in *Plasmodium* liver stage infection. The siRNA Cul3#1 was reverse-transfected into Huh7 cells and 36h later cells were infected with sporozoites. Infection was analyzed by qRT-PCR 48h after sporozoite addition. Data represent mean ± SD of two independent experiments (A). Microscopy analysis revealed that the total number of parasites at 48h post-infection is decreased (B). Schizont size was not significantly altered (C). Representative images of parasites at 48 h post-infection in Neg control and siRNA Cul3#1 stained with anti-Hsp70 antibody. Scale bars: 5 µm (D).

Taken together, our results suggest that depletion of Cullin 3 by siRNA affects *Plasmodium* infection levels at 48 hpi. However, further experiments are necessary to confirm and elucidate the mechanism behind the effect of depletion of Cullin 3 in the infection by *Plasmodium*.

To evaluate the effect of Cullin 3 depletion in the accumulation of vesicles (endolysosomes) around the parasite we performed a microscopy analysis of transfected Huh7 cells, infected with *P. berghei* sporozoites. Cells were stained for parasite anti-Hsp70 (cytosol) and anti-UIS4 (PVM) antibodies and for late endosomes and lysosomes, using anti-LAMP1 antibody. Raw integrated density was measured with ImageJ. We observed no significant differences in vesicle aggregation around the parasite and in the host cell cytosol when the cells are depleted of Cullin 3 (Figure 12).

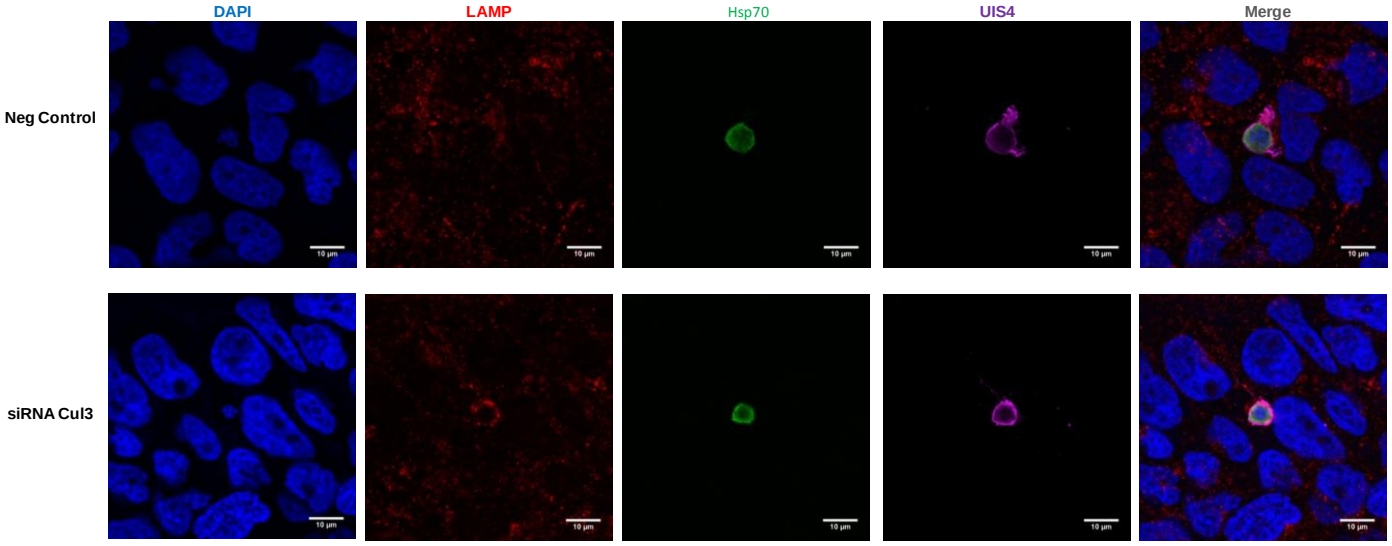

Figure 12: Effect of depletion of Cullin 3 in the accumulation of vesicles around the parasite. Huh7 cells transfected with SiRNA oligo infected with Pb sporozoites were stained with anti-LAMP1 (red), anti-HSP7 (parasite cytoplasm; green) and anti-UIS4 (PVM marker; magenta) antbodies. Nuclei were stained with DAPI (blue). Scale bars: 10 µm.

The cellular and molecular interactions that occur between the malaria parasite and the host liver cell remain largely unknown. Currently, studies reveal a novel *Plasmodium* – host cellular interaction, where host vesicles from the endolysosomal pathway could be important for schizont development (Lopes da Silva *et al.*, 2012). Lopes da Silva and colleagues suggest two alternative hypotheses for the presence of the vesicles around the parasite, either act as a host defense mechanism, or alternatively, that they could somehow be used by the parasite for its own benefit, possibly as a rich source of nutrients (Lopes da Silva *et al.*, 2012). Recently, Cullin 3 has been identified as a regulator of endocytic pathway. Depletion of Cullin 3 resulted in the deformation of late endosome and a defect in the transport of endocytic cargo to lysosomes (Huotari *et al.*, 2012). Our results suggest that host Cullin 3 is important for *Plasmodium* infection in hepatoma cells, however no significant alterations are observed in the distribution or accumulation of vesicles around the parasite upon Cullin 3 depletion. The endosome maturation process after cargo uptake at the plasma membrane involves several distinct steps, including morphological changes, exchange of membrane components, movement of the endosomes, a Rab switch, formation of intraluminal vesicles (ILVs), a drop in luminal pH and acquisition of lysosomal components. Cullin 3-mediated ubiquitination could directly or indirectly affect any of these processes (Kim *et al.*, 2011), which can explain why we did not see any alterations in vesicle accumulation. Therefore, further studies should be performed in order to better understand how Cullin 3 signaling influences *Plasmodium* infection.

5. CONCLUSION

In this thesis we proposed to characterize the role of Cullin 3 during *Plasmodium* intra-hepatic development. Although gain-of-function experiments and treatment with the CRLs activation inhibitor MLN4924 were inconclusive, our results showed that Cullin 3 is apparently relevant in the context of malaria infection. In fact, depletion of Cullin 3 expression by siRNA reduced *Plasmodium* levels in Huh7 cells, suggesting that Cullin 3 signaling is important during liver-stage infection. However, more studies are necessary to confirm this phenotype and elucidate the molecular mechanisms behind it. Nevertheless, our results also showed that accumulation of vesicles around the parasite was not altered upon Cullin 3 depletion. The exact role of Cullin 3-mediated ubiquitination in the endocytic pathway still needs to be defined. Further understanding of the players that directly or indirectly affect any of the endosome maturation processes may be important to clarify the interaction between *Plasmodium* parasite and the host cell, therefore to develop new strategies to control malaria liver-stage infection.

6. REFERENCES

Albuquerque, S.S., Carret, C., Grosso, A.R., Tarun, A.S., Peng, X., Kappe, S.H.I., Prudêncio, M., and Mota, M.M. (2009). Host cell transcriptional profiling during malaria liver stage infection reveals a coordinated and sequential set of biological events. BMC Genomics *10*, 270.

Amino, R., Thiberge, S., Martin, B., Celli, S., Shorte, S., Frischknecht, F., and Ménard, R. (2006). Quantitative imaging of Plasmodium transmission from mosquito to mammal. Nat. Med. *12*, 220–224.

Andérica-Romero, A.C., González-Herrera, I.G., Santamaría, A., and Pedraza-Chaverri, J. (2013). Cullin 3 as a novel target in diverse pathologies. Redox Biol. *1*, 366–372.

Bano, N., Romano, J.D., Jayabalasingham, B., and Coppens, I. (2007). Cellular interactions of Plasmodium liver stage with its host mammalian cell. Int. J. Parasitol. *37*, 1329–1341.

Bennett, E.J., Rush, J., Gygi, S.P., and Harper, J.W. (2010). Dynamics of cullin-RING ubiquitin ligase network revealed by systematic quantitative proteomics. Cell *143*, 951–965.

Blank, J.L., Liu, X.J., Cosmopoulos, K., Bouck, D.C., Garcia, K., Bernard, H., Tayber, O., Hather, G., Liu, R., Narayanan, U., *et al.* (2013). Novel DNA damage checkpoints mediating cell death induced by the NEDD8-activating enzyme inhibitor MLN4924. Cancer Res. *73*, 225–234.

Brownell, J.E., Sintchak, M.D., Gavin, J.M., Liao, H., Bruzzese, F.J., Bump, N.J., Soucy, T. a, Milhollen, M. a, Yang, X., Burkhardt, A.L., *et al.* (2010). Substrate-assisted inhibition of ubiquitin-like protein-activating enzymes: the NEDD8 E1 inhibitor MLN4924 forms a NEDD8-AMP mimetic in situ. Mol. Cell *37*, 102–111.

Chen, Z.J., and Sun, L.J. (2009). Nonproteolytic functions of ubiquitin in cell signaling. Mol. Cell *33*, 275–286.

Fontenille, D., and Simard, F. (2004). Unravelling complexities in human malaria transmission dynamics in Africa through a comprehensive knowledge of vector populations. Comp. Immunol. Microbiol. Infect. Dis. *27*, 357–375.

Franke-Fayard, B., Trueman, H., Ramesar, J., Mendoza, J., van der Keur, M., van der Linden, R., Sinden, R.E., Waters, A.P., and Janse, C.J. (2004). A Plasmodium berghei reference line that constitutively expresses GFP at a high level throughout the complete life cycle. Mol. Biochem. Parasitol. *137*, 23–33.

Frevert, U., Engelmann, S., Zougbédé, S., Stange, J., Ng, B., Matuschewski, K., Liebes, L., and Yee, H. (2005). Intravital observation of Plasmodium berghei sporozoite infection of the liver. PLoS Biol. *3*, e192.

Gallup, J.L., and Sachs, J.D. (2001). The Economic Burden of Malaria. 85–96.

Grant, B.D., and Donaldson, J.G. (2009). Pathways and mechanisms of endocytic recycling. Nat. Rev. Mol. Cell Biol. *10*, 597–608.

Greenwood, G.L., Paul, J.P., Pollack, L.M., Binson, D., Catania, J.A., Chang, J., Humfleet, G., and Stall, R. (2005). GREENWOOD *ET AL.* RESPOND. Am. J. Public Health *95*, 929–a–930.

Guerin, P.J., Olliaro, P., Nosten, F., Druilhe, P., Laxminarayan, R., Binka, F., Kilama, W.L., Ford, N., and White, N.J. (2002). Malaria: current status of control, diagnosis, treatment, and a proposed agenda for research and development. Lancet Infect. Dis. *2*, 564–573.

Hershko, A., and Ciechanover, A. (1998). The ubiquitin system. Annu. Rev. Biochem. *67*, 425–479.

Heussler, V., and Doerig, C. (2006). In vivo imaging enters parasitology. Trends Parasitol. *22*, 192–5; discussion 195–6.

Hubner, M., and Peter, M. (2012). Cullin-3 and the endocytic system: New functions of ubiquitination for endosome maturation. Cell. Logist. *2*, 166–168.

Huotari, J., Meyer-Schaller, N., Hubner, M., Stauffer, S., Katheder, N., Horvath, P., Mancini, R., Helenius, A., and Peter, M. (2012). Cullin-3 regulates late endosome maturation. Proc. Natl. Acad. Sci. U. S. A. *109*, 823–828.

Isberg, R.R., O'Connor, T.J., and Heidtman, M. (2009). The Legionella pneumophila replication vacuole: making a cosy niche inside host cells. Nat. Rev. Microbiol. *7*, 13–24.

Jia, L., Li, H., and Sun, Y. (2011). Induction of p21-dependent senescence by an NAE inhibitor, MLN4924, as a mechanism of growth suppression. Neoplasia *13*, 561–569.

Kabeya, Y., Mizushima, N., Ueno, T., Yamamoto, A., Kirisako, T., Noda, T., Kominami, E., Ohsumi, Y., and Yoshimori, T. (2000). LC3, a mammalian homologue of yeast Apg8p, is localized in autophagosome membranes after processing. EMBO J. *19*, 5720–5728.

Kappe, S.H.I., and Duffy, P.E. (2006). Malaria liver stage culture: in vitro veritas? Am. J. Trop. Med. Hyg. *74*, 706–707.

Kim, W., Bennett, E.J., Huttlin, E.L., Guo, A., Li, J., Possemato, A., Sowa, M.E., Rad, R., Rush, J., Comb, M.J., *et al.* (2011). Systematic and quantitative assessment of the ubiquitin-modified proteome. Mol. Cell *44*, 325–340.

Lin, J.J., Milhollen, M.A., Smith, P.G., Narayanan, U., and Dutta, A. (2010). NEDD8-targeting drug MLN4924 elicits DNA rereplication by stabilizing Cdt1 in S phase, triggering checkpoint activation, apoptosis, and senescence in cancer cells. Cancer Res. *70*, 10310–10320.

Lopes da Silva, M., Thieleke-Matos, C., Cabrita-Santos, L., Ramalho, J.S., Wavre-Shapton, S.T., Futter, C.E., Barral, D.C., and Seabra, M.C. (2012). The host endocytic pathway is essential for Plasmodium berghei late liver stage development. Traffic *13*, 1351–1363.

Lu, A., and Pfeffer, S.R. (2013). Golgi-associated RhoBTB3 targets cyclin E for ubiquitylation and promotes cell cycle progression. J. Cell Biol. *203*, 233–250.

Luo, Z., Yu, G., Lee, H.W., Li, L., Wang, L., Yang, D., Pan, Y., Ding, C., Qian, J., Wu, L., *et al.* (2012). The Nedd8-activating enzyme inhibitor MLN4924 induces autophagy and apoptosis to suppress liver cancer cell growth. Cancer Res. *72*, 3360–3371.

Marín, I. (2009). Diversification of the cullin family. BMC Evol. Biol. *9*, 267.

Matsuoka, H., Yoshida, S., Hirai, M., and Ishii, A. (2002). A rodent malaria, Plasmodium berghei, is experimentally transmitted to mice by merely probing of infective mosquito, Anopheles stephensi. Parasitol. Int. *51*, 17–23.

Méresse, S., Steele-Mortimer, O., Finlay, B.B., and Gorvel, J.P. (1999). The rab7 GTPase controls the maturation of Salmonella typhimurium-containing vacuoles in HeLa cells. EMBO J. *18*, 4394–4403.

Milhollen, M.A., Traore, T., Adams-Duffy, J., Thomas, M.P., Berger, A.J., Dang, L., Dick, L.R., Garnsey, J.J., Koenig, E., Langston, S.P., *et al.* (2010). MLN4924, a NEDD8-activating enzyme inhibitor, is active in diffuse large B-cell lymphoma models: rationale for treatment of NF-{kappa}B-dependent lymphoma. Blood *116*, 1515–1523.

Milhollen, M.A., Narayanan, U., Soucy, T.A., Veiby, P.O., Smith, P.G., and Amidon, B. (2011). Inhibition of NEDD8-activating enzyme induces rereplication and apoptosis in human tumor cells consistent with deregulating CDT1 turnover. Cancer Res. *71*, 3042–3051.

Mizushima, N. (2004). Methods for monitoring autophagy. Int. J. Biochem. Cell Biol. *36*, 2491–2502.

Mota, M.M., Pradel, G., Vanderberg, J.P., Hafalla, J.C., Frevert, U., Nussenzweig, R.S., Nussenzweig, V., and Rodríguez, A. (2001). Migration of Plasmodium sporozoites through cells before infection. Science *291*, 141–144.

Mukhopadhyay, D., and Riezman, H. (2007). Proteasome-independent functions of ubiquitin in endocytosis and signaling. Science *315*, 201–205.

Nebenführ, A., Ritzenthaler, C., and Robinson, D.G. (2002). Brefeldin A: deciphering an enigmatic inhibitor of secretion. Plant Physiol. *130*, 1102–1108.

Petroski, M.D. (2010). Mechanism-based neddylation inhibitor. Chem. Biol. *17*, 6–8.

Petroski, M.D., and Deshaies, R.J. (2005). Function and regulation of cullin-RING ubiquitin ligases. Nat. Rev. Mol. Cell Biol. *6*, 9–20.

Pickart, C.M., and Eddins, M.J. (2004). Ubiquitin: structures, functions, mechanisms. Biochim. Biophys. Acta *1695*, 55–72.

Pines, J., and Lindon, C. (2005). Proteolysis: anytime, any place, anywhere? Nat. Cell Biol. *7*, 731–735.

Prudêncio, M., and Mota, M.M. (2007). To migrate or to invade: those are the options. Cell Host Microbe *2*, 286–288.

Prudêncio, M., Rodriguez, A., and Mota, M.M. (2006). The silent path to thousands of merozoites: the Plasmodium liver stage. Nat. Rev. Microbiol. *4*, 849–856.

Prudêncio, M., Rodrigues, C.D., Ataíde, R., and Mota, M.M. (2008). Dissecting in vitro host cell infection by Plasmodium sporozoites using flow cytometry. Cell. Microbiol. *10*, 218–224.

Sachs, J., and Malaney, P. (2002). The economic and social burden of malaria. Nature *415*, 680–685.

Van de Sand, C., Horstmann, S., Schmidt, A., Sturm, A., Bolte, S., Krueger, A., Lütgehetmann, M., Pollok, J.-M., Libert, C., and Heussler, V.T. (2005). The liver stage of Plasmodium berghei inhibits host cell apoptosis. Mol. Microbiol. *58*, 731–742.

Schnatwinkel, C., Christoforidis, S., Lindsay, M.R., Uttenweiler-Joseph, S., Wilm, M., Parton, R.G., and Zerial, M. (2004). The Rab5 effector Rabankyrin-5 regulates and coordinates different endocytic mechanisms. PLoS Biol. *2*, E261.

Sherman, I. W. (1998). *Malaria: parasite biology, pathogenesis, and protection*. *ASM Press* (Vol.4, p. 575). ASM Press. Washington D.C.

Sigismund, S., Argenzio, E., Tosoni, D., Cavallaro, E., Polo, S., and Di Fiore, P.P. (2008). Clathrin-mediated internalization is essential for sustained EGFR signaling but dispensable for degradation. Dev. Cell *15*, 209–219.

Soucy, T.A., Smith, P.G., Milhollen, M.A., Berger, A.J., Gavin, J.M., Adhikari, S., Brownell, J.E., Burke, K.E., Cardin, D.P., Critchley, S., *et al.* (2009). An inhibitor of NEDD8-activating enzyme as a new approach to treat cancer. Nature *458*, 732–736.

Stanway, R.R., Mueller, N., Zobiak, B., Graewe, S., Froehlke, U., Zessin, P.J.M., Aepfelbacher, M., and Heussler, V.T. (2011). Organelle segregation into Plasmodium liver stage merozoites. Cell. Microbiol. *13*, 1768–1782.

Stogios, P.J., Downs, G.S., Jauhal, J.J.S., Nandra, S.K., and Privé, G.G. (2005). Sequence and structural analysis of BTB domain proteins. Genome Biol. *6*, R82.

Sturm, A., Amino, R., van de Sand, C., Regen, T., Retzlaff, S., Rennenberg, A., Krueger, A., Pollok, J.-M., Menard, R., and Heussler, V.T. (2006). Manipulation of host hepatocytes by the malaria parasite for delivery into liver sinusoids. Science *313*, 1287–1290.

Swords, R.T., Kelly, K.R., Smith, P.G., Garnsey, J.J., Mahalingam, D., Medina, E., Oberheu, K., Padmanabhan, S., O'Dwyer, M., Nawrocki, S.T., *et al.* (2010). Inhibition of NEDD8-activating enzyme: a novel approach for the treatment of acute myeloid leukemia. Blood *115*, 3796–3800.

Tanga, M.C., Ngundu, W.I., Judith, N., Mbuh, J., Tendongfor, N., Simard, F., and Wanji, S. (2010). Climate change and altitudinal structuring of malaria vectors in south-western Cameroon: their relation to malaria transmission. Trans. R. Soc. Trop. Med. Hyg. *104*, 453–460.

Vergne, I., Chua, J., Lee, H.-H., Lucas, M., Belisle, J., and Deretic, V. (2005). Mechanism of phagolysosome biogenesis block by viable Mycobacterium tuberculosis. Proc. Natl. Acad. Sci. U. S. A. *102*, 4033–4038.

Warrell, D.A., and Gilles, H.M. (2002). Essential malariology. 352.

Wimuttisuk, W., and Singer, J.D. (2007). The Cullin3 ubiquitin ligase functions as a Nedd8-bound heterodimer. Mol. Biol. Cell *18*, 899–909.

World-Health-Organization (2013). World Malaria Report.

Wu, J., Lin, H., Hu, Y., and Chien, C. (2005). Neddylation and Deneddylation Regulate Cul1 and Cul3 Protein Accumulation. 55–56.

Xirodimas, D.P., Sundqvist, A., Nakamura, A., Shen, L., Botting, C., and Hay, R.T. (2008). Ribosomal proteins are targets for the NEDD8 pathway. EMBO Rep. *9*, 280–286.

Zhao, Y., Xiong, X., Jia, L., and Sun, Y. (2012). Targeting Cullin-RING ligases by MLN4924 induces autophagy via modulating the HIF1-REDD1-TSC1-mTORC1-DEPTOR axis. Cell Death Dis. *3*, e386.

7. APPENDIX

Appendix I: Primers, siRNA sequences and antibodies.

Table 1: Primers used in qRT-PCR experiments

Gene name	Reverse	Forward
Cullin 3	ATG CTG GAG TGT GAG CTG TC	ACG ACA GGA TAT TGG CCC AC
Pb 18S rRNA	GGA GAT TGG TTT TGA CGT TTA TGT G	AAG CAT TAA ATA AAG CGA ATA CAT CCT TAC
hHPRT	CAAGACATTCTTTCCAGTTAAAGTTG	TTTGCTGACCTGCTGGATTAC

Table 2: siRNA sequences

Sequence ID	SiRNA ID#	Sequence, sense 5´-3´	Seguence, antisense 5´-3´
Cul3#1	139189	GCU UGG AAU GAU CAU CAA Att	UUU GAU GAU CAU UCC AAG Ctt
Cul3#2	217187	GCU AUG GUG AUG AUU AGA Gtt	CUC UAA UCA UCA CCA UAG Ctg
Cul3#3	139188	GCU CUA CAC UGG ACU AAG Att	UCU UAG UCC AGU GUA GAG Ctt

Table 3: Antibodies.

Primary Antibodies	Dilution
Anti-Hsp70	1:200
Anti-UIS4	1:1000
Anti-LC3	1:200
Anti-LAMP	1:200
Anti-Myc	1:200
Anti-Cul3	1:300
Secondary Antibodies and dyes	**Dilution**
Anti-mouse Alexa 488	1:400
Anti-Rabbit Alexa 594	1:400
Anti-Goat Alexa 555	1:400
Anti-Goat Alexa 633	1:400
Anti-Rabbit Alexa 647	1:400

DAPI	1:1000

Appendix II: Gating strategy for flow cytometry analysis of infected cells